Gait & Posture 125 (2026) 110102

Contents lists available at ScienceDirect

Gait & Posture

journal homepage: www.elsevier.com/locate/gaitpost

Full length article

Design, mechanical evaluation, and wear trial of 3D printed insole for plantar off-loading in older adults with diabetes

Karolyn Ning [a,b,1], Mei-Ying Kwan [a,1], Kit-Lun Yick [a,b,*]

[a] School of Fashion and Textiles, The Hong Kong Polytechnic University, Hong Kong
[b] Laboratory for Artificial Intelligence in Design, Hong Kong

ARTICLE INFO

Keywords:
Biomechanics
Product design
Prototyping
Aging
Diabetic Foot

ABSTRACT

Background: Up to 15 % of people with diabetes are at risk of developing a foot ulcer. Diabetic insoles are crucial for preventing foot ulcers by redistributing plantar pressure and increasing contact area. This study investigated the effects of novel insoles made with three-dimensional (3D) printed auxetic structure in older adults with diabetes.

Research question: What are the effects of insoles on plantar off-loading, pressure distribution and mechanical properties in older adults with diabetes, as evaluated using a novel 3D printed auxetic-structured insole and compared to conventional insoles?

Methods: Twenty-three elderly patients with diabetes were recruited as research subjects to evaluate the plantar off-loading effect of the insole prototype while walking. A total of seven 3D printed reentrant structures with varying internal angles and beam sizes were fabricated and evaluated. The differences in foot contact area and plantar pressure distribution were compared with conventional insoles. The mechanical properties of the heel pad material, especially its force absorption and compression properties were also evaluated.

Results: The mean peak pressure (MPP) has been reduced by using diabetic insoles during walking. Compared to the commercial diabetic insole, the 3D printed insole shows a reduction of MPP up to 30.7 % which is also able to maintain the most evenly distributed plantar pressure by a 19.7 % increase of contact area with the midfoot.

Significance: The capability of 3D printing on making insoles with 3D geometries that fit the human plantar surface was confirmed. The proposed 3D printed insole reliably alleviates peak plantar pressure based on laboratory findings and future long-term follow-up studies are necessary to confirm these benefits in daily life activities. The output of the study could also extend to the development of customized insole orthosis to prevent the development of diabetic foot ulcers.

1. Introduction

Diabetes is a growing global health challenge that affects a large population, with up to 15 % of people with diabetes developing foot ulcers in their lifetime [1,2]. In the United States, diabetic foot ulcers cost approximately $1.38 billion per year for wound care and account for more than 80 % of amputations [3]. Diabetes is a major factor of accelerated atherosclerosis and leads to an increase in elastic shear stiffness and a reduction in wound healing ability. This raises the risk of foot ulcers in patients with diabetes [4–6]. Diabetic insoles are crucial for preventing foot ulcers by redistributing pressure through increased contact area [7,8]. Diabetic insoles should achieve a peak plantar pressure of less than 200 kPa and facilitate over 80 % treatment adherence [9].

To enhance fit and increase contact area, molding is commonly used to produce custom-made insoles [10–12]. However, the choice of materials is limited, conventional materials like moldable foams can reduce the peak plantar pressure to 300 kPa, but the likelihood of foot ulcer development and recurrence remains high. Moldable foams have low permeability and tend to trap heat. This creates a humid environment that favors the growth of pathogenic bacteria and fungi, potentially increasing skin vulnerability and the likelihood of foot tissue damage [13–15]. Recently, three-dimensional (3D) printing has been introduced to provide a flexible choice in material dimension, structure, hardness,

* Corresponding author at: School of Fashion and Textiles, The Hong Kong Polytechnic University, Hong Kong.
E-mail address: tcyick@polyu.edu.hk (K.-L. Yick).
[1] Karolyn Ning and Mei-Ying Kwan have equal authorship

https://doi.org/10.1016/j.gaitpost.2026.110102
Received 20 July 2025; Received in revised form 1 December 2025; Accepted 18 January 2026
Available online 21 January 2026

and mass [16]. 3D printed insoles have been shown to improve the microclimate within the shoe and significantly reduce foot pain by enhancing fit [17,18].

Recent advancements in materials science have led to increased investigation of auxetic materials, characterized by their negative Poisson's ratio. This property results in contraction under uniaxial compression and expansion under uniaxial stretch [19]. Research has demonstrated that these materials exhibit superior compression and force absorption [20–22]. Unlike conventional materials, auxetic structures distribute loads over a larger surface area, which effectively reduces peak force [22]. These advantages indicate potential for the application of auxetic structures in diabetic insole design to reduce plantar peak pressure. The advent of 3D printing technology has provided a manufacturing route for producing insoles with auxetic components.

Scholars have proposed auxetic heel pad and midsole to enhance shock absorption capabilities. Compared to conventional insole materials, the peak contact force and mean pressure of auxetic heel pad were reduced by 10 % and 14 %, respectively [23,24]. However, previous studies relied on finite element simulations and lacked testing with patients, limiting their clinical relevance. Given the superior mechanical properties of auxetic structure, this study aims to explore their responses and effects through a wear trial and to provide new insights into diabetes management by systematically analyzing relevant data from patients with diabetes.

This study demonstrates the development and application of a half-insole featuring an arch pad and auxetic heel pad using stereolithography (SLA) and selective laser sintering (SLS) 3D printing. The dimension of the arch pad can be tailored according to the plantar geometry. The study highlights the development of diabetic insoles using 3D printing. The effects of the proposed insoles on fit, plantar pressure distribution in older adults with diabetes will be investigated by wear trial. The mechanical properties of the insole materials, including the force absorption and compression properties, will also be analyzed.

2. Material and methods

2.1. 3D printed auxetic structures for heel pad cushioning

A total of seven 3D printed reentrant structures with varying internal angles and beam sizes were fabricated and evaluated. Table 1 lists the material specifications and specimens. SLA and SLS printing enable the fabrication of complex 3D auxetic structures without support materials, ensuring accurate model structures [23]. Resin (Flexible 80 A, Elastic 50 A), and thermoplastic polyurethane (TPU) (Flexa Bright, FS 1092 A) were chosen for printing the 3D auxetic reentrant structures with a beam size of 1.3 mm (Samples A, B, C, and D). In addition, 3D models with internal angles of 60° (auxetic) and 90° (non-auxetic) were printed using TPU (FS 1092 A). The beam sizes for auxetic Samples D and F were 1.3 mm and 2 mm, respectively, while the beam sizes for non-auxetic Samples E and G were 1.4 mm and 2.2 mm, respectively.

Three conventional insole materials, including double-layered ethylene-vinyl acetate (EVA) foam, EVA foam, and polyurethanes (PU) were compared. Their mechanical properties were evaluated in terms of force absorption and hysteresis energy loss during compression, to determine their suitability as a heel pad for force reduction.

The impact force reduction percentage of the samples was measured using a modified ASTM D2632 Standard Test Method for Rubber Property - Resilience by Vertical Rebound based on Lo et al. [25]. A Voltage Mode Integrated Electronics Piezo-Electric force sensor, made of stainless steel and designated Model 1051V5 (Dytran Instruments Inc., U.S.A.), was employed to measure dynamic forces. This sensor has a sensitivity of 5.13 mV/Lb.F. Voltage measurements were conducted using the MonoDAQ Data Acquisition device (DEWESoft® company, Slovenia).

This test simulates the insole materials under sudden force. The measurement of impact force was done by using a dynamic load cell mounted on a baseplate. A sample was placed on top of the load cell, and a 64 g ball was dropped vertically from a height of 40 cm, guided by a plunger, to assess the impact force on the load cell.

The force reduction ability of the sample is the percentage reduction in peak force after the sample is placed on the load cell. The degree of impact force reduction reflects the insole's effectiveness in protecting the foot from unexpected shocks or gait termination. Eq. (1) was used to calculate the force reduction ability:

$$FR_x = (1\text{-}F_x/F_o) \times 100\% \quad (1)$$

where FR_x is the force reduction percentage (%) of the sample, F_x is the peak force measured for the specimen (N), and F_o is the peak force measured for the ground surface (N).

Hysteresis energy loss is also measured in accordance with ASTM D3574 Foam Hysteresis Energy Loss Testing, which is defined as the difference between the loading and unloading energies expressed as a percentage of the loading energy. This test evaluates load-bearing performance and quantifies the material's tendency to impart a reaction force onto the plantar surface. It shows the deformation behavior of the material during unloading after axial compression and also shows the tendency to impart a reaction force onto the plantar surface between mid-stance and toe-off. Larger hysteresis energy loss shows lower reaction force applied on the plantar surface. The specimens were compressed under a load of 800 N and the energy lost during unloading was calculated by using Eq. (2):

$$HL = [(\beta - \mu) \times 100]/\ \beta \quad (2)$$

where HL is the hysteresis energy loss percentage (%) of the sample, β is the loading energy, and μ is the unloading energy.

2.2. Insole samples for dynamic walking trials

Based on the optimal reentrant structure design, a multi-layered insole prototype (Insole X) was developed. The standardized insole shape was developed based on foot morphology observed from the participant foot scans, including footprint and arch shape, and also incorporated features from commercially available insoles. Insole X features an auxetic heel pad, a spacer fabric and a PU layer to enhance cushioning and reduce plantar pressure [26]. A honeycomb arch pad was designed by using AutoCAD 3D modelling software (Autodesk Inc., San Francisco, California). Fig. 1 shows the structural design of Insole X. The height of the arch pad (1.86 mm) was tailored-made based on 3D foot scans. This enhances the fit of insoles with plantar geometry, an important approach for reducing excessive pressure and facilitating plantar pressure redistribution [7,27].

The off-loading performance of the prototype (Insole X) was compared to EVA foam insole (Insole Y). Insole Y is a commercially available diabetic insole (Inocep®) that also features a heel cup and arch pad. Fig. 2 shows the photos of the two insoles. Both insoles were tested in sports shoes using the Pedar®-x system (Novel Electronics Inc., Pittsburgh, Pennsylvania) to measure plantar pressure in the toes, forefoot, midfoot, and rearfoot. Participants were instructed to walk ten times on an eight-meter-long walkway at self-selected walking speed to measure their mean walking speed (Brower Timing Systems, Draper, Utah). They were then required to walk on the walkway with each insole sample at a speed of ± 10 % of the mean of self-selected walking speed to minimize the effect of speed variation on the plantar pressure. Three successful walking trials were collected for each condition. To eliminate the effects of acceleration and deceleration during the initiation and termination of each walking trial, the middle three steps were extracted for analysis. All participants were required to wear a pair of sports shoes with permeable shoe upper made of mesh spacer fabric, and a pair of standardized socks made of a blend of cotton, polyester, and spandex during testing to minimize confounding variables.

Table 1
Material specifications.

Sample	Material	STL model	Printing method	Structure	Beam size (mm)	Density (g/cm^3)	Thickness (mm)	Internal angle
A	Resin (Flexible 80A)	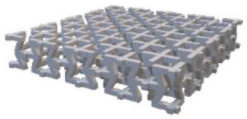	SLA	Auxetic	1.3	0.206	8.86	60°
B	Resin (Elastic 50A)	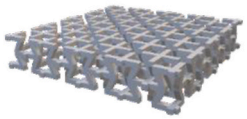	SLA	Auxetic	1.3	0.227	8.60	60°
C	TPU (Flexa Bright)	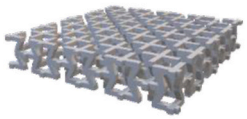	SLS	Auxetic	1.3	0.125	8.96	60°
D	TPU (FS 1092A)	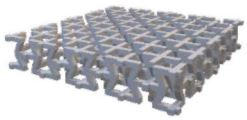	SLS	Auxetic	1.3	0.178	9.52	60°
E	TPU (FS 1092A)	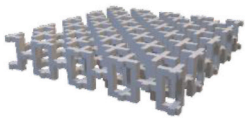	SLS	Non-auxetic	1.4	0.152	8.76	90°
F	TPU (FS 1092A)	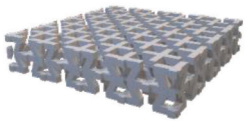	SLS	Auxetic	2.0	0.301	10.02	60°
G	TPU (FS 1092A)	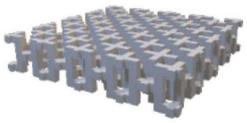	SLS	Non-auxetic	2.2	0.295	10.22	90°
H	EVA foam (INOCEP®)	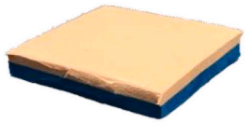	/	/	/	0.127	8.56	/
I	EVA foam (Nora® Lunalastik)		/	/	/	0.189	9.36	/
J	PU (PORON®)	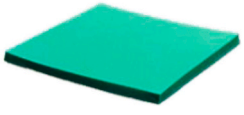	/	/	/	0.532	9.42	/

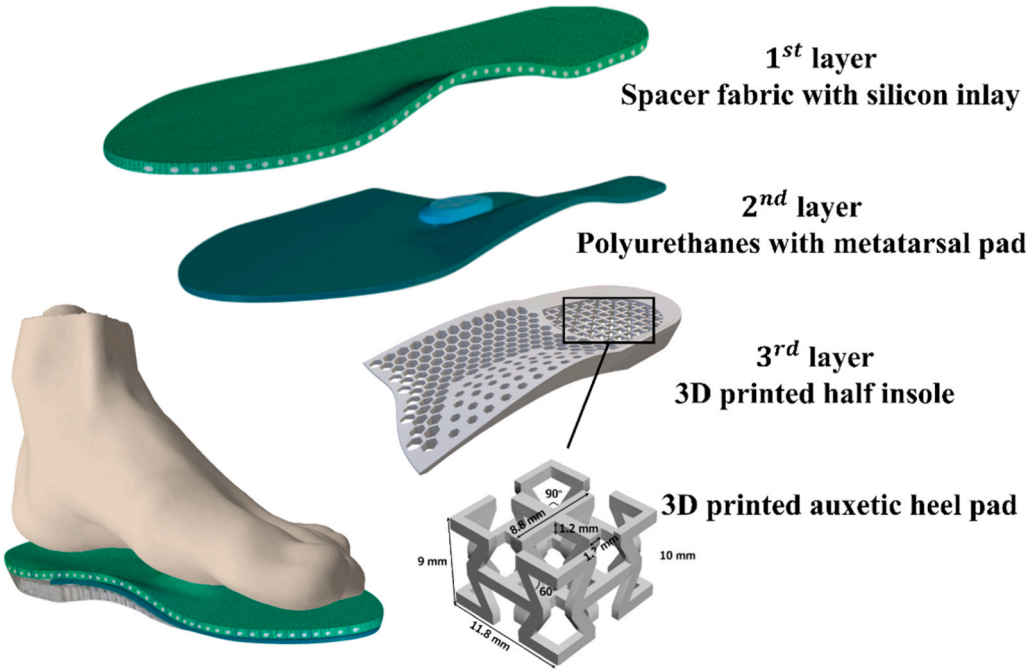

Fig. 1. Structural design of multi-layered insole prototype Insole X.

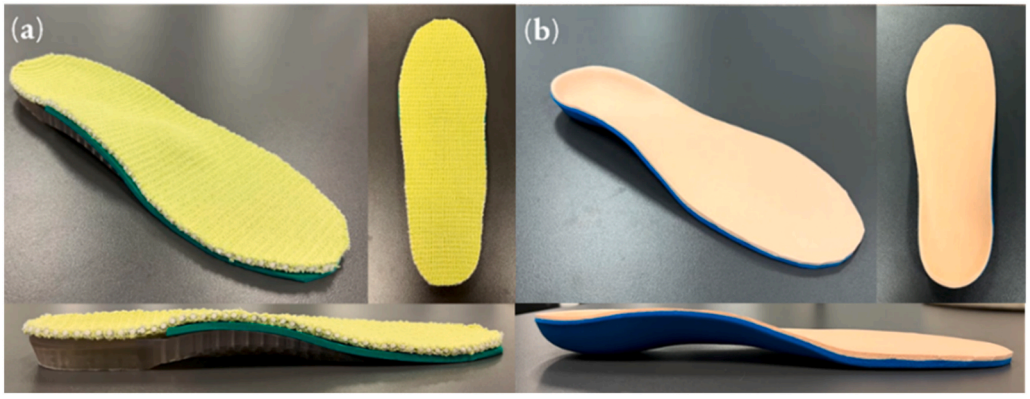

Fig. 2. The 3D, top, and medial side views of (a) Insole X, and (b) Insole Y.

2.3. Participants

Twenty-three elderly patients with diabetes were invited to take part in the wear trial. The inclusion criteria included: (a) age between 50 and 70 years old, (b) diagnosis of Type 1 or Type 2 diabetes, (c) no balance impairment, (d) the ability to walk along an eight-meter-long walkway at least five times without assistance, (e) no current or previous history of foot ulcer, and (f) foot size between EU 38–39. To recruit participants, a foot care program was conducted to collect information from patients with diabetes about their foot problems and the need for diabetic foot orthoses through foot measurements and questionnaires. Static and dynamic balance abilities were also assessed using Berg Balance Scale40 by therapists. The experiment was approved by the Human Subjects Ethics Sub-Committee of the Hong Kong Polytechnic University (HSEARS20200128001). All the participants provided informed written consent before participating in the study.

2.4. Data processing

The plantar mean peak pressure (MPP) and its percentage reduction during walking for the two insole samples were compared with those without insoles, and the change in contact area between the insole and the plantar surface was also analyzed. The reduction of mean peak pressure and change of contact area using the insole conditions were calculated by using Eqs. (3) and (4) below:

$$\text{RMPP} = [(MPP_i - MPP_N)/\ MPP_N] \text{ x } 100\% \quad (3)$$

where RMPP is the reduction of MPP (%), MPP_i is the mean peak pressure using the insole condition, and MPP_N is the mean peak pressure without the insole.

$$\Delta\text{CoA} = [(CoA_i - CoA_N)/\ CoA_N] \text{ x } 100\% \quad (4)$$

where ΔCoA is the change in the contact area between insole and plantar (%), CoA_i is the contact area using the insole condition, and CoA_N is the contact area without the insole.

2.5. Statistical analysis

All parameters were tested for normal distribution by using the Shapiro-Wilk test. The statistical analysis was processed by using the Statistical Package for the Social Sciences program (International

Business Machines Corporation, Armonk, New York), with significance set at $p < 0.05$. The repeated measures analysis of variance (ANOVA) was conducted to evaluate the effect of the insole conditions for each measurement point in terms of the actual value and reduction of plantar MPP, actual value, and change of contact area. Wilcoxon signed-rank tests were conducted for post hoc pairwise comparisons following ANOVA. The comparisons included: (1) Insole X vs. Insole Y, (2) Insole X vs. No Insole, and (3) Insole Y vs. No Insole.

3. Results

3.1. Clinical characteristics and demographics

The study population included twenty-three patients with Type 2 diabetes (21 females and 2 males) with a mean age of 66.3 ± 5.9 years, Body Mass Index (BMI) of 23.9 ± 2.8 kg/m^2, height of 157.5 ± 4.3 cm, body mass of 58.5 ± 5.2 kg, and diabetes duration of 13.4 ± 12.4 years, reflecting a significant history of managing this chronic condition. All participants have no foot ulcer or balance impairment. This specific population requires targeted intervention and monitoring to prevent potential complications associated with diabetes. A post-hoc power analysis was conducted using G*Power 3.1.9.7 (Heinrich Heine University Düsseldorf, Düsseldorf, Germany) based on the achieved sample size of 23. The analysis demonstrated that the study had a high power (>0.95) to detect large effects (f ≥ 0.35).

3.2. Force absorption and compression properties of heel pad materials

The force reduction results of the samples are plotted in Fig. 3(a). The auxetic 3D printed sample B made of resin (86.90 %) offers the highest reduction of force, followed by auxetic 3D printed sample D made of TPU (86.65 %). Force reduction ability of conventional samples H, I and J are 74.35 %, 79.88 %, and 82.38 %, respectively. The results showed that the 3D printed materials can reduce force better than conventional insole material.

In addition, the materials were subjected to compression with 800 N of force. The hysteresis energy loss was calculated and plotted in Fig. 3 (c), and the force-strain curves were plotted in Fig. 3(d). The auxetic sample A (73.50 %) made of Flexible 80 A resin showed the most significant loss of hysteresis energy during the compression test, followed by auxetic sample D (59.42 %), and sample C (56.97 %).

3.3. Plantar peak pressure dynamics in walking

After assessing the force absorption ability, compression properties and hysteresis energy loss, prototype Insole X, constructed from a 3D printed half-insole featuring an auxetic structure made with Flexible 80 A resin, was subsequently prepared for wear trial. The MPP at the toes, forefoot, midfoot, and rearfoot were measured during walking under various insole conditions and compared to a no-insole condition, as illustrated in Fig. 4(a).

At the toe region, Insole X demonstrated a plantar MPP of 201 kPa, significantly lower than that of Insole Y (236 kPa) and the no-insole

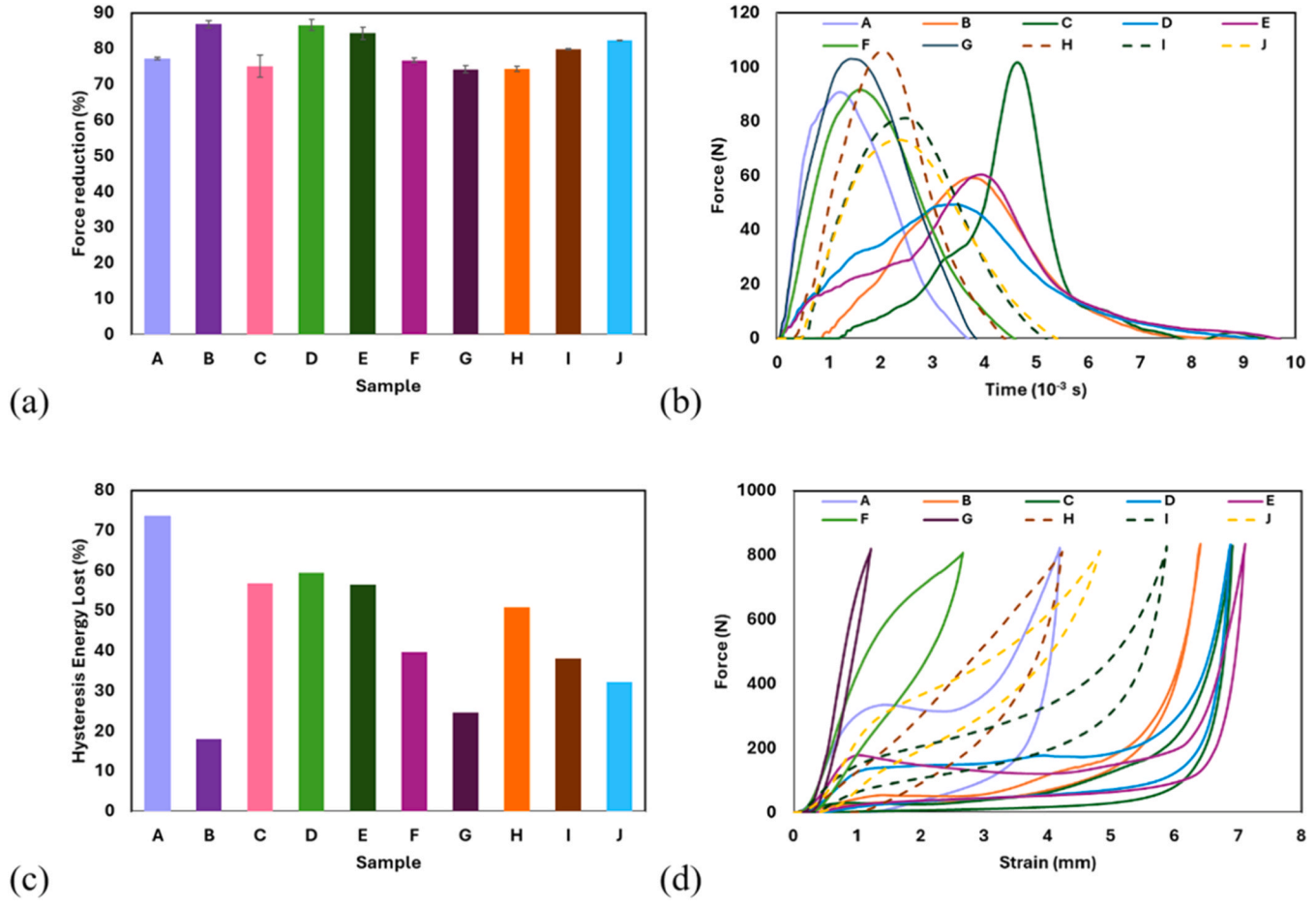

Fig. 3. (a) Impact force reduction of the 3D printed materials (A to G) and conventional insole materials (H to J), (b) force-time curves of the 3D printed materials and conventional insole materials, (c) hysteresis energy loss during compression, and (d) stress-strain curves during compression. Note: Error bars show the standard error

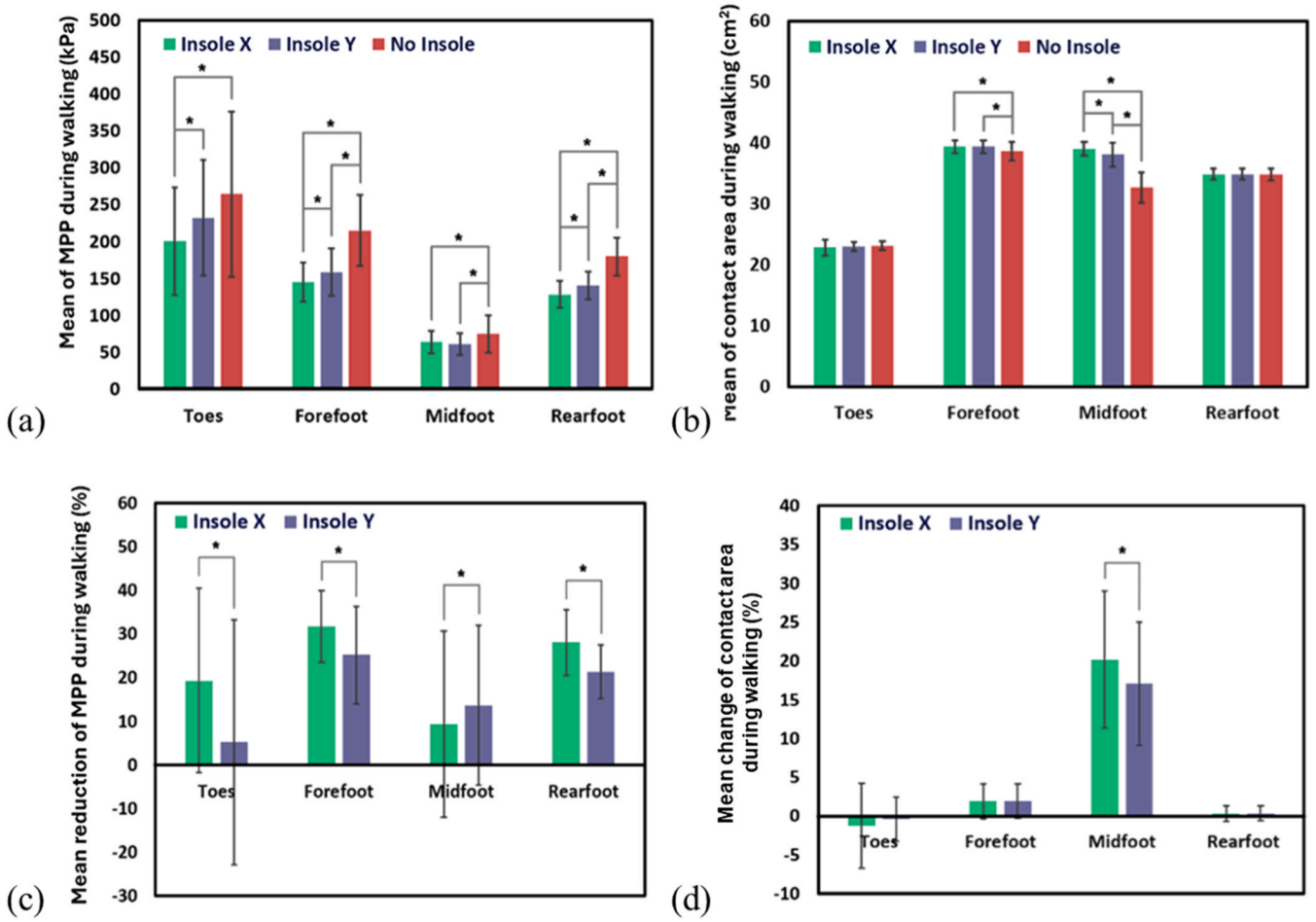

Fig. 4. (a) Mean peak pressure during walking, (b) mean contact area during walking, (c) mean reduction of peak pressure during walking with use of insole samples, and (d) mean change of contact area during walking with use of insole samples. Note: The significance level was set at $p < 0.05$; Error bars show the standard error.

condition (264 kPa). Significant differences were also observed at the forefoot with the use of insoles as opposed to the no-insole condition ($Z = -2.521$, $p = 0.012$).

As for the midfoot, the results of the Wilcoxon signed-rank tests revealed a significantly higher MPP when walking without an insole compared to using Insoles X ($Z = -1.965$, $p = 0.049$) and Y ($Z = -2.392$, $p = 0.017$). A lower MPP was recorded for Insole Y (61 kPa) than for Insole X (64 kPa).

Additionally, a significantly lower MPP was observed at the rearfoot with the use of Insole X ($Z = -2.24$, $p = 0.025$), and Insole Y ($Z = -2.521$, $p = 0.012$), as opposed to the no-insole condition. Insole X exhibited significantly lower plantar MPP at the forefoot (145 kPa) and rearfoot (129 kPa).

4. Discussion

4.1. Force absorption and compression properties of heel pad materials

The plotted force-time curves of the materials shown in Fig. 3(b) showed that 3D printed samples B, D, and E have flat peak curves with a long reaction time. The materials that show a longer reaction time can better offset the load [25]. This is favorable for the diabetic insole that the force from unexpected shocks and gait termination can be buffered accordingly.

The auxetic structure shows a higher hysteresis energy loss than the non-auxetic structure during compression. The negative Poisson's property achieved by the auxetic structure results in significant lateral expansion when stretched and lateral contraction when compressed [19]. This distinct behavior enables the materials to distribute and dissipate energy more effectively, significantly affecting their hysteretic behavior [28].

An interesting effect of the auxetic properties can be observed in Fig. 3(d). Auxetic 3D printed materials exhibit longer plastic regions, while non-auxetic conventional insole materials have almost no plastic region and enter the densification region soon after the yield point. The longer plastic region indicates that the auxetic materials can endure greater stress deformation before reaching the breaking point. This feature helps improve energy absorption and comfort. When the rearfoot strikes the ground, the auxetic structure of the Insole X is able to respond more adaptively to the forces exerted, minimizing the peak pressures that are often associated with conventional insoles. This dynamic response not only enhances comfort but also promotes a more natural gait by reducing excessive concentrations of pressure in specific regions. Conventional materials tend to become stiffer after reaching their yield point, and their rapid transition to densification may not be able to fully adapt to the dynamic movement of the foot during activities, resulting in an uncomfortable experience for the user.

4.2. Plantar peak pressure dynamics in walking

Peak plantar pressure in the forefoot was significantly reduced when the insole was used compared to the no-insole condition. This suggests that the insole not only provides cushioning but also helps redistribute load. By providing contoured support, insoles can improve load

distribution across the forefoot, thereby reducing peak pressure specifically at the metatarsal heads. This observed effect is consistent with previous studies [29,30]. In diabetic foot care, the forefoot is a common site for ulceration, and these results suggest that the insoles can effectively reduce the load on this high-risk area, making them a key component of preventive diabetic foot care.

In the midfoot, the MPP of insole X is higher than that of insole Y. This may be because the arch pad of insole X adopts a 3D scanning geometry structure, which makes the arch pad fit more closely to the foot arch and increases the contact area, which helps to disperse and reduce the MPP of other foot regions. The redistribution of forces not only reduces peak pressures at rearfoot but also helps increase the overall comfort of the insole during prolonged use [31,32]. This bespoke fitting is particularly important for patients with diabetes, as minor reduction in plantar pressure can significantly reduce the risk of ulceration [23].

Insole X exhibited significantly lower plantar MPP at the forefoot and rearfoot, indicating its efficacy in reducing plantar pressure and promoting even distribution. Insole X incorporates an auxetic structure in the heel pad, allowing it to expand laterally when compressed, creating a more distributed pressure response, allowing the insole to better adapt to the movement of walking. The lower MPP achieved by Insole X in the rearfoot further improves comfort and reduces risk of foot-related issues. Previous studies have shown that patients with severe neuropathy experience significantly elevated rearfoot pressures, a key factor in ulcer formation [33]. Relieving this specific elevated pressure offsets a primary mechanism of tissue destruction, thereby reducing ulcer risk. This reduced pressure also alleviates the discomfort associated with excessive loading, thereby improving comfort. In comparison, EVA insoles, while providing some cushioning, have limited ability to distribute plantar pressure and adapt to foot movements [34]. The resilience and cushioning effect provided by EVA are insufficient to prevent the sharp pressure gradients that can precipitate ulceration [35].

The off-loading performance of Insole X and Insole Y was also compared with the percentage reduction of MPP at all foot regions depicted in Fig. 4(c). The repeated measures ANOVA indicated a significantly higher reduction of MPP by using Insole X at the toes, forefoot, and rearfoot compared to Insole Y. Specifically, Insole X showed a 19.4 % reduction at the toes, which is higher than Insole Y (6.08 %). This suggests that Insole X provides better cushioning and support in the toe region, which is crucial during the push-off phase of walking. At the forefoot, Insole X is capable of reducing 30.7 % of MPP, while the MPP reduction of Insole Y is 24.6 %. Similarly, the MPP reduction of 27.2 % at the rearfoot after using Insole X was also higher than the MPP reduction of 20.7 % after using Insole Y. By minimizing pressure, Insole X may have potential to prevent the formation of calluses, blisters, and ulcers.

4.3. Foot contact area analysis in walking

The contact area between the insole and the plantar surface while walking at the toes, forefoot, midfoot, and rearfoot is illustrated in Fig. 4 (b). Pairwise comparisons at the forefoot, significant differences were found between the presence and absence of insoles ($p < 0.05$). The contact area of midfoot was significantly increased after using the insoles. This might be associated with the 3D geometry of the insole, which conforms to the plantar shape of the midfoot and helps to bear the load to reduce MPP in other foot regions. The geometry of the arch support is critical for this increased contact area, facilitating the redistribution of plantar pressure from the high-pressure regions to the low-pressure regions [7,8]. Therefore, the pressure in other plantar regions is transferred to midfoot, resulting in a relatively lower MPP reduction, as shown in Fig. 4(c).

In addition, significant differences were observed among all three conditions at the midfoot ($p < 0.05$). Insole X increased the midfoot contact area by 19.7 %, which was significantly greater than the 16.7 % increase seen with Insole Y ($p < 0.05$). This may be due to their difference in material compression properties. Since the auxetic structure in Insole X exhibited lower hysteresis energy losses, they deformed less under pressure, which helped maintain a stable contact area during walking. This allows the insole to distribute pressure more evenly, providing better cushioning and support, which can enhance the overall efficiency of energy transfer during movement.

The results shown in Fig. 4(d) confirm that the proposed insole prototype provides effective reduction of plantar pressure during walking. The increased contact area provided by 3D printed auxetic structures contributes to reduced peak plantar pressure, thereby reducing the risk of heel ulceration [23,36,37].

5. Conclusions

This study demonstrates the potential of 3D printed auxetic structures for enhancing off-loading performance compared to conventional materials. The 80 A resin auxetic heel pad reduced rearfoot pressure by 12.7 %, while the proposed Insole X achieved a 30.7 % reduction in MPP at the toes and rearfoot and a 19.7 % larger midfoot contact area, promoting even pressure distribution. Although MPP at the toes slightly exceeded the 200 kPa ideal threshold, the results suggest strong potential for ulcer prevention.

Various foot deformities in patients with diabetes may considerably affect the plantar pressure distribution. Further research could involve wear trials on individuals with different foot conditions. Durability assessments through repeated compression test are also recommended to understand the ability of recovery under longer-term repeated use.

The generalizability of our findings is limited by the gender imbalance in the study cohort. Although these results are highly relevant to older females with Type 2 diabetes, they should be extrapolated to male patients with caution. Future research should recruit balanced samples or conduct sex-stratified analyses to confirm whether the observed effects are consistent across genders.

Overall, the findings suggest that 3D printing technologies and auxetic structures offer promising applications for insole developing, providing an alternative material choice that enhances wear comfort and pressure distribution. This research could pave the way for customized insoles to prevent diabetic foot ulcers.

CRediT authorship contribution statement

Mei-Ying Kwan: Writing – review & editing, Writing – original draft, Visualization, Validation, Formal analysis, Data curation, Conceptualization. **Kit-Lun Yick:** Writing – review & editing, Supervision, Software, Resources, Project administration, Funding acquisition, Conceptualization. **Karolyn Ning:** Writing – original draft, Validation, Methodology, Investigation, Formal analysis, Data curation, Conceptualization.

Funding

This work was supported by the Laboratory for Artificial Intelligence in Design, the InnoHK initiative of the Innovation and Technology Commission of the Hong Kong Special Administrative Region Government, and The Hong Kong Polytechnic University [grant number YWET].

Declaration of Competing Interest

The authors declared no potential conflicts of interest with respect to the research, authorship, and/or publication of this article.

References

[1] S. Ahmed, A. Barwick, P. Butterworth, S. Nancarrow, Footwear and insole design features that reduce neuropathic plantar forefoot ulcer risk in people with diabetes: a systematic literature review, J. Foot Ankle Res. 13 (2020) 30, https://doi.org/10.1186/s13047-020-00400-4.

[2] A.J.M. Boulton, The diabetic foot: from art to science. The 18th Camillo Golgi lecture, Diabetologia 47 (2004) 1343–1353, https://doi.org/10.1007/s00125-004-1463-y.
[3] C.W. Hicks, S. Selvarajah, N. Mathioudakis, R.E. Sherman, K.F. Hines, J. H. Black III, C.J. Abularrage, Burden of infected diabetic foot ulcers on hospital admissions and costs, Ann. Vasc. Surg. 33 (2016) 149–158, https://doi.org/10.1016/j.avsg.2015.11.025.
[4] A. Gefen, M. Megido-Ravid, M. Azariah, Y. Itzchak, M. Arcan, Integration of plantar soft tissue stiffness measurements in routine MRI of the diabetic foot, Clin. Biomech. 16 (2001) 921–925, https://doi.org/10.1016/S0268-0033(01)00074-2.
[5] S. Pai, W.R. Ledoux, The shear mechanical properties of diabetic and non-diabetic plantar soft tissue, J. Biomech. 45 (2012) 364–370, https://doi.org/10.1016/j.jbiomech.2011.10.021.
[6] N.C. Schaper, J.J. Van Netten, J. Apelqvist, B.A. Lipsky, K. Bakker, Prevention and management of foot problems in diabetes: a summary guidance for daily practice 2015, based on the IWGDF guidance documents, Diabetes Metab. Res. Rev. 32 (2016) 7–15, https://doi.org/10.1002/dmrr.2695.
[7] S.A. Bus, J.S. Ulbrecht, P.R. Cavanagh, Pressure relief and load redistribution by custom-made insoles in diabetic patients with neuropathy and foot deformity, Clin. Biomech. 19 (2004) 629–638, https://doi.org/10.1016/j.clinbiomech.2004.02.010.
[8] J.J. Van Netten, P.A. Lazzarini, D.G. Armstrong, S.A. Bus, R. Fitridge, K. Harding, L. F. Reed, Diabetic Foot Australia guideline on footwear for people with diabetes, J. Foot Ankle Res. 11 (2018) 2, https://doi.org/10.1186/s13047-017-0244-z.
[9] R. Waaijman, M. De Haart, M.L.J. Arts, D. Wever, A.J. Verlouw, F. Nollet, S.A. Bus, Risk factors for plantar foot ulcer recurrence in neuropathic diabetic patients, Diabetes Care 37 (2014) 1697–1705, https://doi.org/10.2337/dc13-2470.
[10] S.A. Bus, R. Haspels, T.E. Busch-Westbroek, Evaluation and optimization of therapeutic footwear for neuropathic diabetic foot patients using in-shoe plantar pressure analysis, Diabetes Care 34 (2011) 1595–1600, https://doi.org/10.2337/dc10-2206.
[11] N.A. Guldemond, P. Leffers, N.C. Schaper, A.P. Sanders, F. Nieman, P. Willems, G. Walenkamp, The effects of insole configurations on forefoot plantar pressure and walking convenience in diabetic patients with neuropathic feet, Clin. Biomech. 22 (2007) 81–87, https://doi.org/10.1016/j.clinbiomech.2006.08.004.
[12] J.B.J. Zwaferink, W. Custers, I. Paardekooper, H.A. Berendsen, S.A. Bus, Optimizing footwear for the diabetic foot: data-driven custom-made footwear concepts and their effect on pressure relief to prevent diabetic foot ulceration, PLoS ONE 15 (2020) e0224010, https://doi.org/10.1371/journal.pone.0224010.
[13] S. Bagavathiappan, J. Philip, T. Jayakumar, B. Raj, P.N.S. Rao, M. Varalakshmi, V. Mohan, Correlation between plantar foot temperature and diabetic neuropathy: a case study by using an infrared thermal imaging technique, J. Diabetes Sci. Technol. 4 (2010) 1386–1392, https://doi.org/10.1177/193229681000400613.
[14] K. Moulaei, M. Malek, A. Sheikhtaheri, A smart wearable device for monitoring and self-management of diabetic foot: a proof of concept study, Int. J. Med. Inf. 146 (2021) 104343, https://doi.org/10.1016/j.ijmedinf.2020.104343.
[15] T.P. Rajan, L.D. Souza, G. Ramakrishnan, G.M. Zakriya, Comfort properties of functional warp-knitted polyester spacer fabrics for shoe insole applications, J. Ind. Text. 45 (2016) 1239–1251, https://doi.org/10.1177/1528083714557056.
[16] P.E. Chatzistergos, A. Gatt, C. Formosa, K. Farrugia, N. Chockalingam, Optimised cushioning in diabetic footwear can significantly enhance their capacity to reduce plantar pressure, Gait Posture 79 (2020) 244–250, https://doi.org/10.1016/j.gaitpost.2020.05.009.
[17] T. Tarrade, F. Doucet, N. Saint-Lô, M. Llari, M. Behr, Are custom-made foot orthoses of any interest on the treatment of foot pain for prolonged standing workers? Appl. Erg. 80 (2019) 130–135, https://doi.org/10.1016/j.apergo.2019.05.013.
[18] K. Ning, K.L. Yick, A. Yu, J. Yip, Effects of textile-fabricated insole on foot skin temperature and humidity for enhancing footwear thermal comfort, Appl. Ergon. 104 (2022) 103803, https://doi.org/10.1016/j.apergo.2022.103803.
[19] X. Ren, R. Das, P. Tran, T.D. Ngo, Y.M. Xie, Auxetic metamaterials and structures: a review, Smart Mater. Struct. 27 (2018) 023001, https://doi.org/10.1088/1361-665X/aaa61c.
[20] T. Li, F. Liu, L. Wang, Enhancing indentation and impact resistance in auxetic composite materials, Compos. Part B Eng. 198 (2020) 108229, https://doi.org/10.1016/j.compositesb.2020.108229.
[21] T. Wang, J. An, H. He, X. Wen, X. Xi, A novel 3D impact energy absorption structure with negative Poisson's ratio and its application in aircraft crashworthiness, Compos. Struct. 262 (2021) 113663, https://doi.org/10.1016/j.compstruct.2021.113663.
[22] C. Yang, H.D. Vora, Y. Chang, Behavior of auxetic structures under compression and impact forces, Smart Mater. Struct. 27 (2018) 025012, https://doi.org/10.1088/1361-665X/aa9b44.
[23] M.S.H. Leung, K.L. Yick, Y. Sun, L. Chow, S.P. Ng, 3D printed auxetic heel pads for patients with diabetic mellitus, Comput. Biol. Med. 146 (2022) 105582, https://doi.org/10.1016/j.compbiomed.2022.105582.
[24] Y. Sun, Q. Zhou, W. Niu, S. Zhang, K.L. Yick, B. Gu, S. Zhu, 3D printed sports shoe midsoles: enhancing comfort and performance through finite element analysis of negative Poisson's ratio structures, Mater. Des. 245 (2024) 113292, https://doi.org/10.1016/j.matdes.2024.113292.
[25] W.T. Lo, K.L. Yick, S.P. Ng, J. Yip, New methods for evaluating physical and thermal comfort properties of orthotic materials used in insoles for patients with diabetes, J. Rehabil. Res. Dev. 51 (2014) 311–324, https://doi.org/10.1682/JRRD.2013.01.0012.
[26] T.I. Yi, E.C. Lee, N.H. Son, M.K. Sohn, Comparison of the forefoot pressure-relieving effects of foot orthoses, Yonsei Med. J. 63 (2022) 864–872, https://doi.org/10.3349/ymj.2022.63.9.864.
[27] P.R. Cavanagh, S.A. Bus, Off-loading the diabetic foot for ulcer prevention and healing, Plast. Reconstr. Surg. 127 (2011) 248S–256S, https://doi.org/10.1097/PRS.0b013e3182024864.
[28] W. Ng, H. Hu, Tensile and deformation behavior of auxetic plied yarns, Phys. Status Solidi B 254 (2017) 1600790, https://doi.org/10.1002/pssb.201600790.
[29] M.Y. Kwan, K.L. Yick, J. Yip, C.Y. Tse, The immediate effects of hallux valgus orthoses: a comparison of orthosis designs, Gait Posture 90 (2021) 283–288, https://doi.org/10.1016/j.gaitpost.2021.09.174.
[30] T. Yamamoto, Y. Hoshino, N. Kanzaki, K. Nukuto, T. Yamashita, K. Ibaraki, H. Kato, Plantar pressure sensors indicate women to have a significantly higher peak pressure on the hallux, toes, forefoot, and medial of the foot compared to men, J. Foot Ankle Res. 13 (2020) 1–7, https://doi.org/10.1186/s13047-020-00410-2.
[31] R. Xu, Z. Wang, T. Ma, Z. Ren, H. Jin, Effect of 3D printing individualized ankle-foot orthosis on plantar biomechanics and pain in patients with plantar fasciitis: a randomized controlled trial, Med. Sci. Monit. 25 (2019) 1392–1400, https://doi.org/10.12659/MSM.915045.
[32] K.W. Cheng, Y. Peng, T.L.W. Chen, G. Zhang, J.C.W. Cheung, W.K. Lam, J.T.-M. Cheung, A three-dimensional printed foot orthosis for flexible flatfoot: an exploratory biomechanical study on arch support reinforcement and undercut, Materials 14 (2021) 5297, https://doi.org/10.3390/ma14185297.
[33] A. Caselli, H. Pham, J.M. Giurini, D.G. Armstrong, A. Veves, The forefoot-to-rearfoot plantar pressure ratio is increased in severe diabetic neuropathy and can predict foot ulceration, Diabetes Care 25 (2002) 1066–1071, https://doi.org/10.2337/diacare.25.6.1066.
[34] A. Martínez-Santos, S. Preece, C. Nester, Evaluation of orthotic insoles for people with diabetes who are at-risk of first ulceration, J. Foot Ankle Res. 12 (2019) 1–9, https://doi.org/10.1186/s13047-019-0344-z.
[35] M. Hamedi, P. Salimi, Reducing foot plantar pressure using superelastic nitinol monofilaments as spacer yarns in a novel weft knitted spacer fabric insole, J. Ind. Text. 52 (2022), https://doi.org/10.1177/15280837221127314, 15280837221127314.
[36] R. Kumari, Impact of prefabricated versus 3-D insoles on pain and quality of life in patients with plantar fasciitis, Int. J. Health Sci. Res. 12 (2022) 153–157, https://doi.org/10.52403/ijhsr.20220221.
[37] J. Gerrard, D. Bonanno, G. Whittaker, K. Landorf, Effect of different orthotic materials on plantar pressures: a systematic review, J. Foot Ankle Res. 13 (2020) 35, https://doi.org/10.1186/s13047-020-00401-3.